Punching Shear Design in Flat Slabs: A Comparative Study of Model Code 2020 and the new Eurocode 2

Lorraine Dias Inácio, Mayra Soares Pereira Lima Perlingeiro and Mauro Schulz

Civil Engineering Department,
Federal Fluminense University - UFF,
Av. Passo da Pátria, 156, Niterói, RJ 24210-240, Brazil

Summary

This paper examines the performance of Model Code 2020 (MC2020) and EN 1992-1-1:2023 (EC2–23) in the punching shear design of flat slabs, both with and without shear reinforcement. A database of 67 slab tests, including 29 from Brazil, is analyzed, covering columns in various slab positions. Estimated capacities are compared to experimental values from the literature, providing an assessment of the ratio between experimental and calculated punching shear capacities for each design approach. Results based on MC2020 indicate that estimated capacities are generally accurate, satisfactory, or conservative when compared to experimental data. EC2–23 provides similar predictions for internal columns but tends to overestimate the shear capacity of some edge and corner columns. This discussion supports future updates to the punching shear design recommendations in the Brazilian standard, incorporating the Critical Shear Crack Theory to enhance accuracy and reliability.

1 INTRODUCTION

The punching shear design of flat slabs is a critical aspect of structural engineering. Shear failure around columns due to concentrated stresses can initiate progressive collapse. Accurate prediction of punching shear resistance is essential for ensuring structural safety and cost-effective design. Standards such as ACI 318-19 [1], EN 1992-1-1:2004 [2], NBR 6118:2023 [3], fib Model Code 2020 (MC2020) [4], and the recent EN 1992-1-1:2023 (EC2–23) [5] provide different calculation methods, taking into account variables such as column position, shear reinforcement, and load eccentricity.

This study compares the MC2020 and EC2–23 models for flat slabs with and without shear reinforcement based on 67 experimental tests, including 29 conducted in Brazil. The analysis evaluates the safety levels of each approach and examines differences in calculation coefficients. Given that both models are based on the Critical Shear Crack Theory (CSCT), the study highlights its potential for improving the understanding and modeling of punching shear behavior. The findings seek to refine predictive accuracy and contribute to revising the Brazilian standard's recommendations, enhancing the reliability of structural designs.

2 CRITICAL SHEAR CRACK THEORY

Recent years have seen significant advances in understanding and modeling punching shear failure, with the Critical Shear Crack Theory (CSCT) emerging as a key development in the field [6]. This theory is based on the formation of a critical crack in the slab around the column, which widens and propagates through the slab thickness as the loading increases. The width of this crack is proportional

to the slab rotation (ψ) and effective depth (d), while its roughness, influenced by the maximum aggregate size, affects the final resistance [7]. Based on these principles, the CSCT establishes the following formula for calculating the punching shear resistance of slabs without shear reinforcement:

$$V_{R,c} = \frac{0.75}{1+15\dfrac{\psi d}{d_{g0}+d_g}} b_0 d \sqrt{f_c} \tag{1}$$

In this equation, $V_{R,c}$ represents the punching shear resistance without shear reinforcement; b_0 denotes the control perimeter around the column; d is the effective depth of the slab; $\sqrt{f_c}$ is the concrete compressive strength; ψ is the slab rotation at the column; d_{g0} is the reference aggregate size, assumed to be 16 mm, and d_g is the maximum aggregate size in the concrete.

According to Muttoni and Ruiz [8], when shear reinforcement is included in the design, the total punching shear resistance (V_R) is expressed as the sum of the concrete resistance $(V_{R,c})$ and the additional contribution of the shear reinforcement $(V_{R,s})$, i.e.:

$$V_R = V_{R,c} + V_{R,s} \tag{2}$$

The shear reinforcement contribution is calculated as follows

$$V_{R,s} = \frac{E_{sw}\psi}{6} A_{sw} \le f_{ywd} A_{sw} \tag{3}$$

where E_{sw} is the modulus of elasticity of the shear reinforcement steel, f_{ywd} is the steel yield strength, and A_{sw} is the bar area.

3 CODE PROVISIONS IN PUNCHING SHEAR

This research discusses punching shear resistance verification in slabs according to MC2020 and EC2–23. These codes are based on the Critical Shear Crack Theory. The current NBR 6118:2023 relies on earlier versions of these standards, which adopt a different formulation.

The study examines internal, edge, and corner column configurations. Fig. 1 presents an example of these configurations, illustrating the basic control perimeter $b_{0.5}$ adopted in CSCT for punching shear calculations.

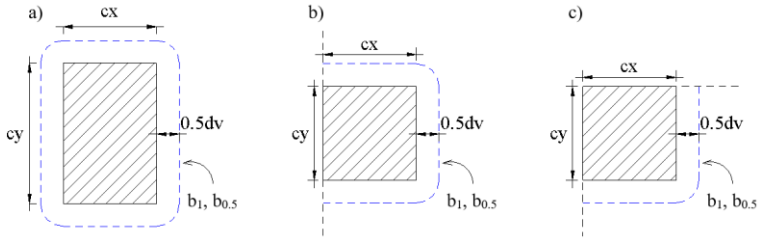

Fig. 1 Basic control perimeter according to MC2020 and EC2–23: a) internal column; b) edge column e c) corner column.

The basic control perimeter for analysis, located at a distance $0.5d_v$ from the column faces, is denoted as b_1 and $b_{0.5}$ in MC2020 and EC2–23, respectively. The control perimeter is reduced when column dimensions exceed $3d_v$, where d_v is the effective depth of the slab. In the cases analysed in this study, d_v always corresponds to the slab's effective depth. The column sides are c_x and c_y in the x and y directions, respectively. In slabs without shear reinforcement, only the concrete contribution is considered.

In slabs with shear reinforcement, its contribution to punching shear capacity is restricted by a maximum allowable value. An additional control perimeter must be verified at a distance of $0.5d_v$ from the outermost reinforcement layer, where the transverse reinforcement contribution is disregarded.

3.1 Model Code 2020 (MC2020)

The design shear resistance and applied forces, respectively denoted as V_{Rd} and V_{Ed}, must satisfy the inequality $V_{Rd} \geq V_{Ed}$.

The value of the concrete contribution $V_{Rd,c}$ is obtained through

$$V_{Rd,c} = k_{\psi} \frac{\sqrt{f_{ck}}}{\gamma_c} b_0 d_v \tag{4}$$

$$k_{\psi} = \frac{1}{1.5 + 0.9 k_{dg} \psi d} \leq 0.6 \tag{5}$$

$$k_{dg} = \frac{32}{16 + d_g} \geq 0.75 \tag{6}$$

The parameter k_{ψ} depends on the slab rotations, k_{dg} is a coefficient related to the aggregate size, and d_g is the maximum aggregate size in the concrete slab. When this value is not provided, $d_g = 9.5\text{mm}$ is assumed. The shear-resistant control perimeter b_0 is determined as

$$b_0 = k_e . b_{1,red} \tag{7}$$

where $b_{1,red}$ is the reduced control perimeter. The factor k_e, which represents the eccentricity coefficient, is discussed in Section 4.

When shear reinforcement is not considered, $V_{Rd} = V_{Rd,c}$.

The portion of punching shear resistance attributed to the shear reinforcement is calculated as:

$$V_{Rd,s} = \left(\Sigma A_{sw}\right) k_e \sigma_{swd} \sin\alpha \tag{8}$$

ΣA_{sw} represents the sum of the areas of all shear reinforcement located in the region between $0.35 d_v$ and d_v from the column face. The stress activated in the shear reinforcement is determined by the following expression:

$$\sigma_{swd} = \frac{E_{sw} \psi}{6} \left(1 + \frac{f_{bd}}{f_{ywd}} \frac{d}{\varphi_w}\right) \leq f_{ywd} \tag{9}$$

where φ_w denotes the diameter of the shear reinforcement. The bond stress f_{bd} is given by $f_{bd} = 1.4 / \gamma_C \left(f_{ck}^{2/3}\right) \leq 5.5 / \gamma_C$. The factors γ_C and γ_S are considered equal to 1 in the verification of experimental results. E_{sw} is the modulus of elasticity of the shear reinforcement steel.

Considering the reinforcement, the punching shear resistance is given by

$$V_{Rd} = V_{Rd,c} + V_{Rd,s} \leq V_{Rd,\max} \tag{10}$$

The maximum punching shear resistance, denoted as $V_{Rd,\max}$, refers to the maximum compressive strength of the concrete strut near the column and is estimated by the following equation:

$$V_{Rd,\max} = k_{sys} k_{\psi} \frac{\sqrt{f_{ck}}}{\gamma_c} b_0 d_V \leq \frac{\sqrt{f_{ck}}}{\gamma_c} b_0 d_V \tag{11}$$

The coefficient k_{sys} accounts for the performance of punching shear reinforcement in controlling shear cracks and confining the compressed struts. It is assumed to be 1 for slabs without shear reinforcement, 2.8 for slabs with stud-type reinforcement, and 2.4 when using stirrups.

MC2020 provides four levels of approximation (LoAs) for calculations, where higher levels offer more precise estimates but involve greater complexity. When detailed information is unavailable, lower levels should be adopted to obtain more conservative results [9]. This article adopts Level of Approximation II (LoA II), in which the slab rotation is

$$\psi = 1.5 \frac{r_s}{d} \frac{f_{yd}}{E_s} \left(\frac{m_{Sd}}{m_{Rd}}\right)^{1.5} \tag{12}$$

The moments per unit length in the support strip, m_{Sd} and m_{Rd}, represent the applied moment and the flexural capacity, respectively. These moments are determined using formulas presented in MC2020 for different column types. The parameter r_s can be estimated based on the spans, where r_{sx} and r_{sy} are the distances from the column axis to the lines where bending moments are zero, in the x and y

directions, respectively. In continuous slabs, it is commonly approximately as $r_{sx} = 0.22 L_x$ and $r_{sy} = 0.22 L_y$, where L_x and L_y are the spans in the x and y directions, respectively. The design yield strength and the modulus of elasticity of the steel are denoted as f_{yd} and E_s, respectively.

3.2 EN 1992-1-1-2023 (EC2–23)

The design shear stress τ_{Ed} is calculated as:

$$\tau_{Ed} = \beta_e \frac{V_{Ed}}{b_{0.5}\, d_v} \tag{13}$$

The eccentricity coefficient β_e is discussed in Section 4.

The punching shear resistance of slabs without shear reinforcement is calculated as

$$\tau_{Rd,c} = \frac{0.6 k_{pb} \left(100 \rho_l f_{ck} \frac{d_{dg}}{d_v}\right)^{\frac{1}{3}}}{\gamma_v} \le \frac{0.5\sqrt{f_{ck}}}{\gamma_v} \tag{14}$$

where γ_v is the safety factor for shear resistance and

$$1 \le k_{pb} = 3.6\sqrt{1 - \frac{b_0}{b_{0.5}}} \le 2.5 \tag{15}$$

In this study, $\gamma_v = 1$ is adopted for the verification of experimental results. k_{pb} is the punching shear gradient enhancement coefficient, and d_{dg} is the parameter describing the roughness of the failure zone, calculated as $d_{dg} = 16\ \text{mm} + D_{lower}$, where D_{lower} is the coarse aggregate diameter (mm). The reinforcement ratio ρ_l is defined as $\rho_l = \sqrt{\rho_{l,x}\, \rho_{l,y}}$, where $\rho_{l,x}$ and $\rho_{l,y}$ are the reinforcement ratios of bonded flexural reinforcement in the x - and y -directions, respectively.

For distances a_p smaller than $8d_v$, the value of d_v used in equation (14) can be replaced by $a_{pd} = \sqrt{(a_p/8)\, d_v}$, where $a_p = \sqrt{a_{p,x}\, a_{p,y}} \ge d_V$. Distances $a_{p,x}$ and $a_{p,y}$ are mesured from the centroid of the control perimeter to the positions where the bending moments $m_{Sd,x}$ and $m_{Sd,y}$ are zero. The value of a_p can also be approximated as $a_p = 0.22L$, where L is the largest of the adjacent spans in the $x-$ or $y-$ direction.

The punching shear resistance in slabs is determined according to

$$\tau_{Rd,cs} = \eta_c \tau_{Rd,c} + \eta_s \rho_w f_{ywd} \ge \rho_w f_{ywd} \tag{16}$$

where ρ_w and f_{ywd} are the reinforcement ratio and the design yield strength of the shear reinforcement, respectively. Coefficients η_s and η_c are given by

$$\eta_s = \frac{d_v}{150\phi_w} + \left(15\frac{d_{dg}}{d_V}\right)^{1/2} \left(\frac{1}{\eta_c k_{pb}}\right)^{3/2} \le 0.8 \tag{17}$$

$$\eta_c = \tau_{Rd,c} / \tau_{Ed} \tag{18}$$

The maximum shear resistance corresponds to

$$\tau_{Rd,\max} = \eta_{sys} \tau_{Rd,c} \tag{19}$$

where η_{sys} is a coefficient dependent on the type of transverse reinforcement. For studs, it is given as

$$\eta_{sys} = 0.7 + 0.63\left(b_0/d_v\right)^{1/4} \ge 1.0 \tag{20}$$

4 ECCENTRICITY FACTOR IN DIFFERENT DESIGN METHODS

Load eccentricities are essential for evaluating punching shear capacity, as columns typically experience bending moments.

MC2020 and EC2–23 use the coefficients k_e and β_e, respectively, to account for shear stress concentration from load eccentricity. EC2-23 defines β_e according to approximated and refined approaches, and here refined is used. Table 1 presents the formulas for these coefficients.

Table 1 Load eccentricity coefficient formulas in MC2020 and EC2–23.

Model Code 2020 (MC2020)	Eurocode (EN 1992-1-1:2023)
$\frac{1}{k_e} = 1 + 1.1\frac{e_u}{b_u}$ (21)	$\beta_e = 1 + 1.1\frac{e_b}{b_b} \geq 1.05$ (22)
with $e_u = \sqrt{e_{ux}^{\ 2} + e_{uy}^{\ 2}}$	internal columns: with $e_b = \sqrt{e_{b,x}^{\ 2} + e_{b,y}^{\ 2}}$ edge columns: with $e_b = 0.5\lvert e_{b,x}\rvert + \lvert e_{b,y}\rvert$ corner columns: with $e_b = 0.27\left(\lvert e_{b,x}\rvert + \lvert e_{b,y}\rvert\right)$ $b_b = \sqrt{b_{b,\min}\, b_{b,\max}}$
e_{ux}, e_{uy} load eccentricity in x- and y- direction b_u diameter of a circle with the same area as the region enclosed by the control perimeter	$e_{b,x}, e_{b,y}$ load eccentricity in x- and y- direction $b_{b,min}, b_{b,máx}$ minimum and maximum width of control perimeter

Eurocode traditionally accounts for the influence of loading eccentricity in column–slab connections by amplifying the design shear force using a factor β_e. EC2-23 provides a closed-form solution for the Critical Shear Crack Theory (CSCT), which differs significantly from the formulation presented in MC2020. In the latter, the coefficient k_e is used in a related manner and corresponds to $1/\beta_e$. Preliminary studies for edge column solutions in EC2-23 are presented in Reference [10], which proposes $e_b = \sqrt{(\alpha e_x)^2 + e_y^2}$ — where the parameter α is evaluated as 0.6 and 1.0. The expression presented in Table 1 for the effective eccentricity e_b, used for corner columns, is proposed in Reference [11].

5 PUNCHING SHEAR TEST DATABASE FROM THE LITERATURE

This study compares the models from MC2020 and EC2–23 with the results of 67 slab-column connection tests, with and without shear reinforcement.

The database includes 30 internal, 22 edge, and 15 corner columns. Connections with and without shear reinforcement are analyzed, covering both continuous and isolated slabs. The selected studies include Oliveira [12], Albuquerque [13] and Albuquerque et al. [14], Zaghlool [15] and Agudelo [16], Stamenkovic [17] and Stamenkovic and Chapman [18].

The shear reinforcement always consists of studs. When the authors do not specify the maximum aggregate size, a median value of 9.5 mm is assumed. The ratios between experimental and code-calculated load capacities are evaluated using routines developed by the authors in the C++ programming language.

6 EXPERIMENTAL RESULTS FROM THE LITERATURE

The punching shear capacities from the codes are compared with experimental data from the database (Table 2). The coefficient λ represents the ratio between the experimental (V_{exp}) and calculated (V_{calc}) punching shear capacities using the theoretical models of MC2020 and EC2–23. The moments along the x- and y-directions are denoted as M_x and M_y, respectively.

Table 2 Results for the set of tests included in the present study.

Reference	Exp.	Case	d [mm]	c_x [mm]	c_y [mm]	V_{exp} [kN]	M_x [kNm]	M_y [kNm]	A_{sw} [cm^2]	λ *MC2020*	λ *EC2–23*
Oliveira (2013)	LN01	Internal	143	400	200	1084	0,00	0,00	0,50	1,34	1,34
	LN02	Internal	143	400	200	1144	0,00	0,00	0,50	1,37	1,35

Reference	Exp.	Case	d [mm]	c_x [mm]	c_y [mm]	V_{exp} [kN]	M_x [kNm]	M_y [kNm]	A_{sw} [cm^2]	λ *MC2020*	λ *EC2–23*
Oliveira (2013)	LN03	Internal	143	400	200	786	0,00	0,00	-	1,36	1,26
	LN04	Internal	143	400	200	966	0,00	0,00	0,31	1,35	1,23
	LN05	Internal	142	400	200	1143	0,00	0,00	1,23	1,20	1,01
	LS01	Internal	143	400	200	425	114,00	0,00	-	1,19	1,07
	LS02	Internal	144	400	200	763	218,00	0,00	0,50	1,52	1,48
	LS03	Internal	142	400	200	775	234,00	0,00	0,50	1,59	1,55
	LS04	Internal	143	400	200	712	183,00	0,00	0,31	1,63	1,46
	LS05	Internal	142	400	200	926	272,00	0,00	1,23	1,60	1,40
	LS06	Internal	143	400	200	926	272,00	0,00	0,79	1,58	1,55
	LW01	Internal	141	200	400	446	124,00	0,00	-	1,32	1,19
	LW02	Internal	143	200	400	711	189,00	0,00	0,50	1,39	1,35
	LW03	Internal	142	200	400	733	195,00	0,00	0,50	1,45	1,41
	LW04	Internal	142	200	400	617	131,00	0,00	0,31	1,33	1,19
	LW05	Internal	142	200	400	815	241,00	0,00	1,23	1,42	1,24
Albuquerque (2014); Albuquerque, Melo and Vollum (2016)	L1	Edge	147	300	300	308	92,00	0,00	-	1,44	1,10
	L2	Edge	146	300	300	315	0,00	0,00	-	1,05	0,96
	L3	Edge	146	300	300	256	-77,00	0,00	-	1,63	1,05
	L4	**Edge**	146	300	300	210	-84,00	0,00	-	1,54	**0,93**
	L5	Edge	146	300	300	374	-37,00	0,00	-	1,56	1,21
	L6	Edge	146	300	300	330	-66,00	0,00	-	1,70	1,18
	L7	Edge	146	300	300	288	-115,00	0,00	-	1,89	1,16
	L8	Edge	146	300	300	320	-128,00	0,00	-	2,17	1,33
	L9	Edge	146	300	300	489	0,00	0,00	0,50	1,71	1,23
	L10	Edge	146	300	300	445	-89,00	0,00	0,50	1,85	1,15
	L11	Edge	146	300	300	304	-110,00	0,00	-	1,99	1,25
	L12	Edge	146	300	300	347	-55,00	0,00	-	1,61	1,18
	L13	Edge	146	300	300	357	-125,00	0,00	-	2,28	1,45
Zaghlool (1973)	Z-I (1)	**Corner**	121	178	178	74,3	19,20	19,20	-	1,21	**0,85**
	Z-II (1)	Corner	121	267	267	137,9	38,50	38,50	-	1,52	1,21
	Z-II (2)	Corner	121	267	267	177,2	53,40	53,40	-	1,80	1,45
	Z-II (3)	Corner	118	267	267	177,9	58,00	58,00	-	1,97	1,50
	Z-II (5)	Corner	121	267	267	148,6	0,00	0,00	-	1,46	1,17
	Z-II (5d)	Corner	121	267	267	137,9	0,00	0,00	-	1,36	1,09
	Z-II (6)	**Corner**	121	267	267	82,3	38,90	38,90	-	1,38	**0,91**
	Z-III (1)	Corner	121	356	356	179,7	52,70	52,70	-	1,58	1,28
Agudelo (2003)	S1	Corner	115	250	250	121,4	37,94	37,94	-	1,61	1,18
	S2	Corner	115	300	300	116,7	37,93	37,93	-	1,37	1,04
	S3	Corner	115	350	350	124,9	42,15	42,15	-	1,40	1,04
Stamenkovic (1969); Stamenkovic and Chapman (1974)	V_I_1	Internal	56	127	127	119,7	0,00	0,00	-	1,28	1,07
	V_I1_1	**Internal**	56	127	127	104,5	0,00	0,00	-	1,13	**0,94**
	V_I2_1	Internal	56	127	127	129,9	0,00	0,00	-	0,98	0,95
	V_I_2	Internal	56	127	127	117,4	0,00	0,00	-	1,43	1,23
	V_Ir_1	Internal	56	152	76	108,5	0,00	0,00	-	1,41	1,25
	V_E_1	Edge	56	127	127	74,7	0,00	0,00	-	1,87	1,36
	V_C_1	**Corner**	56	127	127	27,1	0,00	0,00	-	1,31	**0,89**
	C_I_1	Internal	56	127	127	84,5	7,30	0,00	-	1,37	1,11
	C_I_2	Internal	56	127	127	62,3	10,50	0,00	-	1,42	1,17
	C_I_3	Internal	56	127	127	33,8	13,60	0,00	-	1,37	1,16
	C_I_4	Internal	56	127	127	20,9	16,70	0,00	-	1,44	1,23

Reference	Exp.	Case	d [mm]	c_x [mm]	c_y [mm]	V_{exp} [kN]	M_x [kNm]	M_y [kNm]	A_{sw} [cm^2]	λ $_{MC2020}$	λ $_{EC2-23}$
Stamenkovic (1969); Stamenkovic and Chapman (1974)	C_Ir_1	Internal	56	152	76	85,7	7,30	0,00	-	1,76	1,55
	C_Ir_2	Internal	56	152	76	67,3	10,90	0,00	-	1,65	1,42
	C_Ir_3	Internal	56	152	76	39,9	15,70	0,00	-	1,69	1,48
	C_Ir_4	Internal	56	152	76	21,6	16,80	0,00	-	1,58	1,42
	Ct_E_1	Edge	56	127	127	45,8	0,00	4,90	-	1,39	1,36
	Ct_E_2	Edge	56	127	127	34,9	0,00	5,70	-	1,17	1,24
	Ct_E_3	Edge	56	127	127	23,5	0,00	9,40	-	1,29	1,43
	Ct_E_4	Edge	56	127	127	12,9	0,00	10,10	-	1,17	1,29
	Cn_E_1	Edge	56	127	127	73,2	5,60	0,00	-	1,75	1,29
	Cn_E_2	Edge	56	127	127	54,7	9,20	0,00	-	2,33	1,29
	Cn_E_3	**Edge**	56	127	127	24,9	10,10	0,00	-	2,13	**0,89**
	Cn_E_4	**Edge**	56	127	127	10,9	8,80	0,00	-	1,72	**0,62**
	C_C_1	Corner	56	127	127	24,9	6,20	0,00	-	2,05	1,03
	C_C_2	**Corner**	56	127	127	15,9	6,40	0,00	-	2,05	**0,81**
	C_C_3	**Corner**	56	127	127	8	6,20	0,00	-	1,95	**0,59**
	C_C_4	**Corner**	56	127	127	3,6	5,60	0,00	-	1,62	**0,40**

The prediction ratios have mean values $\lambda_{mean}^{MC2020} = 1.55$ and $\lambda_{mean}^{EC2-23} = 1.18$, corresponding to MC2020 and EC2–23, respectively.

The criteria for evaluating the coefficient λ follow the methodology presented by Oliveira [9]. According to this approach, values with $\lambda < 0.95$ are considered unsafe, while those in the range $0.95 \le \lambda \le 1.15$ are classified as accurate. Values between $1.15 \le \lambda \le 1.30$ are considered satisfactory, and values greater than 1.30 indicate a conservative approach.

Calculations based on MC2020 yield prediction ratios $\lambda \ge 0.98$ for 100% of the analyzed dataset. EC2–23 provides satisfactory results for interior columns, with $\lambda \ge 0.94$ in all cases. However, 9 out of 37 edge and corner columns exhibit $0.40 \le \lambda \le 0.93$. Similarly, Reference [11] reports 7 out of 34 corner columns with $0.67 \le \lambda \le 0.92$ when using the refined β_e-factor.

From a design safety perspective, achieving $V_{exp} / V_{calc} > 0.95$ is generally preferred, as consistently provided by MC2020. Accepting lower values would require a reliability-based safety assessment, especially considering that brittle punching failure at slab–column connections may trigger progressive collapse of the entire structure.

7 CONCLUSIONS

This study presents preliminary results from a comparative analysis of the MC2020 and EC2–23 design formulas for punching shear in flat slabs. Although both standards adopt similar theoretical formulations, they differ in their approach to punching shear verification, with MC2020 defining capacity in terms of design shear forces, whereas EC2–23 adopts a formulation based on shear stresses. More notable differences arise in the eccentricity coefficients, particularly for edge and corner columns.

The punching shear capacities computed according to these standards were compared with experimental data from a database containing 67 test results from the literature. This database includes tests on internal, edge, and corner columns and slabs with and without shear reinforcement. The comparison is based on a coefficient representing the ratio of experimental to calculated punching shear capacities.

Results based on MC2020 indicate consistent and conservative predictions across all cases. EC2–23 provides acceptable estimates for internal columns but tends to yield lower V_{exp} / V_{calc} ratios for some edge and corner columns. Ongoing research has shown that this discrepancy can be reduced by modifying the equations for the effective eccentricity e_b in these cases.

Further investigations are expanding the experimental dataset and assessing the predictive performance of the formulations adopted by MC2020 and EC2–23, which, although both based on the Critical Shear Crack Theory, differ in their specific approaches. This study aims to support future revisions of

NBR 6118 by identifying the formulation that provides more accurate and reliable results for punching shear in flat slabs, particularly at connections with edge and corner columns.

Acknowledgments

The first author acknowledges CAPES for the financial support provided throughout this research.

References

[1] American Concrete Institute. 2019. Building Code Requirements for Structural Concrete and Commentary. ACI 318R-19.

[2] Comité Européen de Normalisation. 2004. Eurocode 2 - Design of Concrete Structures – Part 1-1: General Rules and Rules for Buildings. Stockholm, Sweden: Comité Européen de Normalisation.

[3] Associação Brasileira de Normas Técnicas. 2023. *Design of Concrete Structures – Procedures.* NBR 6118.

[4] fib Model Code for Concrete Structures. 2020. International Federation for Structural Concrete. Lausanne, Switzerland: fib.

[5] EN 1992-1-1:2023. 2023. Eurocode 2: Design of Concrete Structures - Part 1-1: General Rules and Rules for Buildings, Bridges and Civil Engineering Structures.

[6] Abu-Salma, D., Vollum, R. L., and Macorini, L. 2024. "Influence of Flexural Reinforcement Detailing on Punching Shear Resistance at Edge and Corner Columns of Flat Slab Buildings." Structures, Elsevier, 2024: 106024. https://doi.org/10.1016/j.istruc.2024.106024

[7] Muttoni, A. 2008. "Punching Shear Strength of Reinforced Concrete Slabs without Transverse Reinforcement." *ACI Structural Journal* 105(4): 440–450. http://dx.doi.org/10.14359/198588

[8] Fernandez Ruiz, M., and Muttoni, A. 2009. "Applications of Critical Shear Crack Theory to Punching of Reinforced Concrete Slabs with Transverse Reinforcement." *ACI Structural Journal* 106(4): 485–494. http://dx.doi.org/10.14359/566144

[9] Sigrist, V., Bentz, E., Ruiz, M. F., Foster, S., and Muttoni, A. 2013. "Background to the fib Model Code 2010 Shear Provisions–Part I: Beams and Slabs." *Structural Concrete* 14(3): 195–203. https://doi.org/10.1002/suco.201200066

[10] Abu-Salma, D., Vollum, R. L., and Macorini, L. 2021. "Design of Biaxially Loaded External Slab-Column Connections." Engineering Structures 249: 113326. https://doi.org/10.1016/j.engstruct.2021.113326

[11] Abu-Salma, D., Vollum, R. L., and Macorini, L. 2023. "Derivation of Shear Enhancement Factor β Used in FprEN 1992 to Calculate Design Shear Force at Corner Columns of Flat Slabs." Structures, Elsevier 50: 602–614. https://doi.org/10.1016/j.istruc.2023.03.049

[12] Oliveira, M. H. 2013. *Punção em Lajes Lisas com Armadura de Cisalhamento Submetidas a Carregamento Excêntrico e Apoiadas sobre Pilares Retangulares.* PhD diss., Faculdade de Tecnologia, Universidade de Brasília, Brasília. Accessed January 31, 2025. https://repositorio.unb.br/handle/10482/13624.

[13] Albuquerque, N. G. B. 2014. Comportamento das Ligações de Lajes Lisas de Concreto Armado com Pilares de Borda Sujeitas a Excentricidades Interna e Externas. PhD diss., Faculdade de Tecnologia, Universidade de Brasília, Brasília. Accessed January 31, 2025. https://repositorio.unb.br/handle/10482/17442.

[14] Albuquerque, N. G. B., Melo, G. S. S. A., and Vollum, R. L. 2016. "Punching Shear Strength of Flat Slab-Edge Column Connections with Outward Eccentricity of Loading." *ACI Structural Journal* 113(5): 1117–1129. http://dx.doi.org/10.14359/51689156.

[15] Zaghlool, E. E. 1971. *Strength and Behaviour of Corner and Edge Column-Slab Connections in Reinforced Concrete Flat Plates.* Doctoral thesis, University of Calgary, Calgary, Canada. Retrieved January 31, 2025, from https://prism.ucalgary.ca.doi:10.11575/PRISM/13724.

[16] Agudelo, C. C. 2003. *Shear Strength of Slab-Corner Column Connections.* MEng Thesis, Department of Civil Engineering and Applied Mechanics, McGill University, Montreal, 86 pages.

[17] Stamenkovic, A. 1969. *Local Strength of Flat Slabs at Column Heads.* PhD thesis, Imperial College of Science and Technology, University of London, London. Accessed January 31, 2025. https://spiral.imperial.ac.uk/bitstream/10044/1/16718/2/Stamenkovic-A-1970-PhD-Thesis.pdf.

[18] Stamenkovic, A., and Chapman, J. C. 1974. "Local Strength at Column Heads in Flat Slabs Subjected to a Combined Vertical and Horizontal Loading." *Proceedings of the Institution of Civil Engineers* 57: 205–232. http://dx.doi.org/10.1680/iicep.1974.4054.